MULTIPORT NETWORK MODEL FOR EVALUATING RADIATION LOSS AND SPURIOUS COUPLING BETWEEN DISCONTINUITIES IN MICROSTRIP CIRCUITS*

Albert Sabban and K.C. Gupta

Department of Electrical and Computer Engineering

University of Colorado

Boulder, Colorado 80309-0425

Abstract

This paper presents a convenient method for evaluating radiation from microstrip discontinuities. The multiport network model is used to find voltage distribution around discontinuity edges and an equivalent magnetic current model is used to compute the external fields produced. As an example, the results show that for a 90° bend in 50Ω line on 10 mil thick substrate with ε_r = 2.2, the radiation loss is 0.1 dB at 30 GHz. Electromagnetic coupling between two discontinuities is evaluated by finding the currents induced by the fields of one of the discontinuities at the location of the second discontinuity.

Introduction

Because of the open nature of the microstrip configuration, hybrid and monolithic microwave circuits suffer from radiation originating at various geometrical discontinuities. Two consequences of this radiation phenomenon are: additional signal loss in the circuit and undesired interactions between different parts of the circuit due to external electromagnetic coupling. These phenomena become significant in two different situations: first, when attempts are made to increase circuit density in monolithic microwave circuits, more bends and other discontinuities are introduced and spurious electromagnetic coupling increases considerably. Secondly, in microstrip antenna arrays, relatively thicker substrates are used and the feed network printed on the same substrate can result in substantial spurious radiation.

Estimates of the radiation loss from microstrip discontinuities have been attempted previously [1-6]. Most of these results are based on the Poynting vector method developed by Lewin [1]. In this approach, a line current located at the middle of the microstrip line is taken as a source of radiation. Thus the method is applicable to narrow microstrip lines. It has been applied to a 90° bend, a step discontinuity, an open end, a line terminated in an impedance, and a matched symmetrical T-junction. The approach is not easily extendable to more complicated geometries found in practical microwave circuits.

This paper presents a convenient method for estimating radiation from microstrip discontinuities of generalized shapes. A planar multiport network model of the discontinuity configuration and the segmentation method is used to evaluate voltage distribution around the edges of the discontinuity. This voltage distribution is expressed as an equivalent magnetic current line source distribution which is used to calculate the far-zone field (for radiation loss) or the near-field at the location of the other discontinuity for spurious coupling calculations.

* This work has been sponsored by the NSF Industry/University Cooperative Research Center for Microwave/Millimeter-Wave Computer-Aided Design at the University of Colorado.

This approach is suitable for being included in microwave CAD packages. Numerical results have been obtained for radiation from bends, steps and T-junctions and are found to be in reasonable agreement with the Poynting vector results wherever available.

Multiport Network Modeling of Microstrip Discontinuities

Multiport network modeling of discontinuity configurations [7-10] is based on parallel plate waveguide model [11] of microstrip lines. Similar network modeling approach has been used earlier for analysis of microstrip patch antennas [12] and for calculating mutual coupling between microstrip patches [13].

Planar Network Model for Microstrip Discontinuities

The planar circuit model for microstrip discontinuities is derived from the planar waveguide model for microstrip lines [11]. The planar waveguide model consists of two parallel conductors bounded by magnetic walls in the transverse directions. The electric and magnetic fields inside the planar model are uniform along the thickness of the substrate. The width of the waveguide model $W_e(f)$ is made larger than the physical microstrip width in order to account for the fringing fields at the edges and is given by

$$W_e(f) = \frac{\eta_0 h}{Z_0(f)\sqrt{\varepsilon_{re}(f)}} \qquad (1)$$

where $Z_0(f)$ is the characteristic impedance, $\varepsilon_{re}(f)$ is the effective dielectric constant, h is the substrate height and η_0 is the wave impedance in free space.

As the frequency dependences of Z_0 and ε_{re} are incorporated in (1), the dispersion effects get built in the analysis of the discontinuities also. The planar models for discontinuity configuration are obtained by replacing the physical widths of the microstrip lines by effective widths given by (1). The effective dimensions in the discontinuity region are obtained by extrapolating the effective edges for the connecting lines (as shown for a 90° bend in Figure 1a) or having an outward extension equal to that for the adjoining microstrip line (as shown in Figure 1b). The planar modeling approach has been used extensively for characterization and compensation of microstrip discontinuities [7-10].

Figure 1. Planar models for microstrip bends.

CH2725-0/89/0000-0707$01.00 © 1989 IEEE

Multiport Network Model for Evaluating Edge Voltages

In order to evaluate the external fields produced by a microstrip discontinuity, we first obtain voltages at the edges of a microstrip structure. A multiport network model, similar to that developed for microstrip patch antennas [12,13] is employed. For implementing this method, we add a number of open ports at the edges of the discontinuity structure from which the radiation (or spurious external coupling) is being evaluated. This is shown in Figures 2(a) and 2(b) for a right-angled bend and a compensated right-angled bend, respectively.

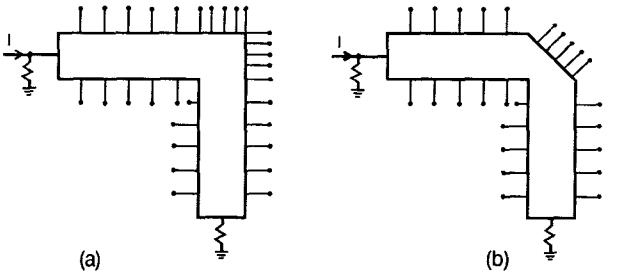

Figure 2. Multiple ports located at the edges of the microstrip discontinuities.

Lengths of transmission lines on two sides of the junction are taken large enough so that the higher order evanescent modes produced by the discontinuities decay out at the locations of external ports 1 and 2. The circuit behavior is simulated by terminating the port 2 in a matched load and adding a matched source to the port 1. Voltages at the N ports at the edges are computed by using the following procedure:

(i) The configuration is broken down in elementary regular segments, connected together at the interfaces by a discrete number of interconnections.

(ii) Z-matrices for each of these elementary segments are evaluated by using the Green's function approach for individual geometries.

(iii) Individual Z-matrices obtained in (ii) are combined together by using the segmentation formula.

(iv) Overall multiport Z-matrix is used for calculating voltages at the N edge ports for a unit current input at the port 1.

As mentioned earlier, a similar procedure has been used for design of microstrip patch antennas [13]. The only distinction in the latter case is the use of edge admittance networks (containing equivalent radiation conductances) which are connected to the edge ports. Because of the non-resonant nature of the microstrip discontinuity structures, the radiated power is small and the edge voltages may be assumed to be unaffected by radiation conductances involved. However, for a more accurate assessment of the radiated power, radiation conductance networks may be added to edge ports and iterative computations may be carried out for evaluating radiation fields.

Evaluation of the Radiated Power

Voltages at the discontinuity edges are represented by equivalent magnetic current sources as shown in Figures 3(a) and 3(b). Each of the magnetic current line sources is divided into small sections over which the field may be assumed to be uniform. The amplitude M of each of the magnetic current elements is twice that of the edge voltage at that location and the phase of M is equal to the phase of the corresponding voltage. The total radiation is computed using the superposition of the far field radiated by each section. Referring to the coordinate system, shown in Figure 4, the far-field

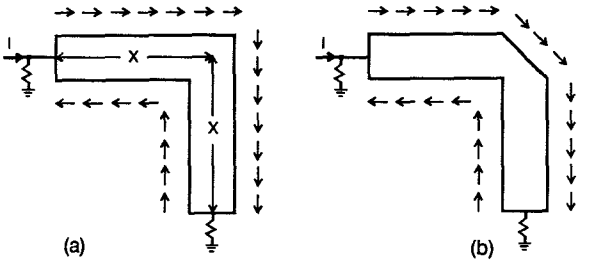

Figure 3. Equivalent magnetic current distribution at discontinuity edges.

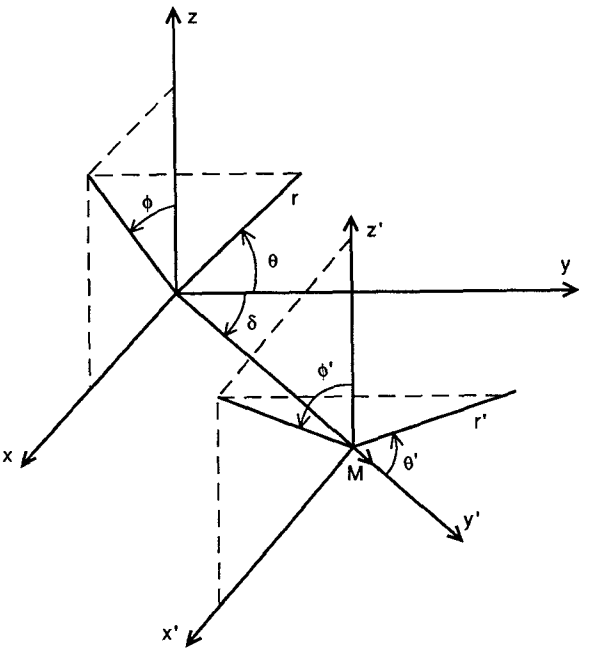

Figure 4. Coordinate system for external field calculations.

pattern may be written in terms of voltages at the various elements. With the voltage at the i-th element as $(V(i)e^{j\alpha(i)})$, we have

$$F(\theta,\phi) = \sum_{i=1}^{N} V(i)\, W(i) \exp\{ (k_0 \gamma_0(i) + \alpha(i) \}\, F_i(\theta,\phi) \qquad (2)$$

where

$$F_i(\theta,\phi) = \frac{\sin\left(\frac{k_0 W(i)}{2}\cos\theta\right)}{\frac{k_0 W(i)}{2}\cos\theta}\sin\theta$$

$$\gamma_0(i) = X_0(i)\sin\theta\cos\phi + Y_0(i)\cos\theta$$

and N is the number of ports, $X_0(i)$, $Y_0(i)$ specify the location of the i-th magnetic current element, and W(i) is the width of the i-th element.

The radiated power is calculated by the integration of the Poynting vector over the half space and may be written as:

$$P_r = \frac{1}{240\pi} \int_{-\pi/2}^{\pi/2} \int_0^{\pi} \left(|E_\theta|^2 + |E_\phi|^2 \right) r^2 \sin\theta \, d\theta \, d\phi \quad (3)$$

The fields E_θ and E_ϕ are expressed in terms of $E(\theta,\phi)$ as:

$$E_\theta = \hat{a}_\theta \, (-2j \, F(\theta, \phi) \, F_\theta) \quad (4)$$

$$E_\phi = \hat{a}_\phi \, (-2j \, F(\theta, \phi) \, F_\phi) \quad (5)$$

$$F_\phi = \sin\phi' \sin\phi + \cos\delta \cos\phi \cos\phi' \quad (6)$$

$$F_\theta = -\sin\phi' \cos\theta \cos\phi + \cos\delta \cos\theta \sin\phi + \sin\delta \cos\phi' \sin\theta \quad (7)$$

$$\cos\theta' = \sin\theta \sin\phi \sin\delta + \cos\theta \cos\delta \quad (8)$$

$$\cos\phi' = \sin\theta \cos\phi / \sqrt{1 - \cos^2\theta'} \quad (9)$$

The radiation loss may be expressed as:

$$\text{Power loss (dB)} = 10 \log_{10}\left(1 - \frac{P_r}{P_i}\right) \quad (10)$$

where P_i is the input power at port 1.

Evaluation of Spurious Coupling Between Two Discontinuities

The spurious coupling between two discontinuities (due to the external fields) may be incorporated in the Multiport Network Model by connecting an additional multiport network between the two discontinuities as shown in Figure 5. The coupling network MCN is characterized in terms of an admittance matrix $[Y_m]$. Elements of this matrix represent mutual admittances between various sections of the edges of the two discontinuities. The terms of the matrix $[Y_m]$ are obtained by representing the edge fields by small sections of length $d\ell$ of equivalent magnetic current and computing the magnetic field (H_θ, H_r) produced at the j-th subsection of the nearby discontinuity. We have

$$H_\theta = j \frac{k_0 M d\ell \sin\theta}{4\pi\eta_0 r} \left(1 + \frac{1}{jk_0 r} - \frac{1}{(k_0 r)^2}\right) e^{-jk_0 r} \quad (11)$$

$$H_r = \frac{M d\ell \cos\theta}{2\pi\eta_0 r^2} \left(1 + \frac{1}{jk_0 r}\right) e^{-jk_0 r} \quad (12)$$

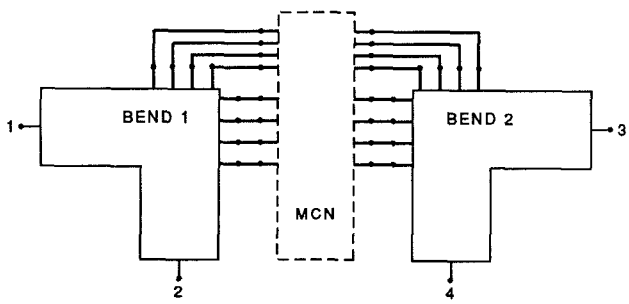

Figure 5. A multiport network (MCN) incorporated for modeling spurious coupling between discontinuities.

The induced current in the j-th element is calculated from the magnetic field as:

$$J_j = (\hat{Z} \times \bar{H}) \cdot \hat{j} \quad (13)$$

where $\hat{j}$ is a unit vector normal to the j-th element. The value of Y_{ji} is obtained from the current induced in the j-th subsection as a result of voltage V_i at the i-th subsection.

$$Y_{ji} = J_j \, d\ell_j / V_i \quad (14)$$

The Z-matrix of the mutual coupling network is the inverse of $[Y_m]$. The segmentation method is used to combine the Z matrix representations of the discontinuities and the coupling network to yield the overall Z matrix. The Z matrix is converted to S-parameters. The effect of the coupling on the circuit performance is obtained from these S-parameters.

It may be noted that a similar procedure has been employed earlier to model the mutual coupling between patches of a microstrip antenna array successfully [13].

Computational Details

Z-Matrix Evaluation

For rectangular planar segments, the impedance matrix elements can be expressed in a single infinite series [14]. The numbers of terms needed for the convergence of the summation was found to be around 100.

The Z matrix elements for sections of transmission line with lengths equal to multiples of half-wavelength become infinitely large. So these line lengths should be avoided. Also for quarter wave sections, some of the Z matrix elements become zero. Thus, for numerical accuracy, it is advisable to avoid quarter wave sections also. The length of each section on either side of the discontinuity should be greater than twice the width of the microstrip line. This allows the higher order evanescent modes to decay out at locations of the external ports (1 and 2 in Figure 2). Also, it is found that to obtain accurate results, the width of the ports at the edges should be less than 0.075 wavelength. Computational results for different widths of interconnected ports were also compared and it is found that the optimum width of interconnected port is about 0.05 wavelength.

In order to identify the regions of the discontinuity configuration that contribute dominantly to the radiated power, several computations were performed by taking different regions around the discontinuity. These computations show that in most of the cases the biggest contribution to the radiated power is due to ports in the region of the discontinuity itself. The results for a right-angled bend, shown in Table 1, illustrate this point.

Table 1: Radiated power as a function of the length of the microstrip line
($\varepsilon_r = 12.9$, $h = 127.1$ μm, $f = 10$ GHz)

Length X (shown in Figure 3)	P_r/P_i *dB*
(0.4 x 0.4) λ	-40.64
(0.35 x 0.35) λ	-40.67
(0.3 x 0.3) λ	-40.77
(0.25 x 0.25) λ	-40.84
(0.2 x 0.2) λ	-41.1
Only ports on bend	-41.1

Radiation from a Right-Angled Microstrip Bend

Results for the power radiated by the 90° bend normalized with respect to the input power is shown in Figure 6 for frequency

ranges from 10 GHz to 40 GHz. These results are in good agreement with results based on the complex Poynting vector method [1], which are also plotted in Figure 6. The radiation loss at 40 GHz is a 0.0062 dB for a 50Ω line bend on GaAs (ε_r = 12.9) substrate. The values for radiation loss from a 90° bend in 50Ω line on a substrate with ε_r = 2.2 at 30 GHz and 40 GHz are 0.1 dB and 0.17 dB, respectively.

Radiation from a Microstrip Step Junction

Power radiated from a step junction discontinuity, change in impedance from 50Ω to 10Ω, on ε_r = 2.2 substrate with thickness of 0.79 mm is plotted in Figure 7. A similar computation for a 50Ω to 70.7Ω junction (at 30 GHz, ε_r = 2.2, thickness 0.02 inch), yields the normalized radiated power to be -24.8 dB when the input power is fed from the 50Ω line and -33 dB when the power is fed from the70.7Ω line.

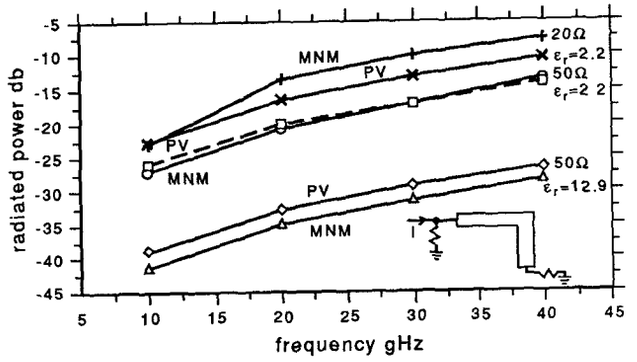

Figure 6. Normalized radiated power from a right angled bend (MNM: Multiport Network Model, and PV: Poynting Vector method [1]).

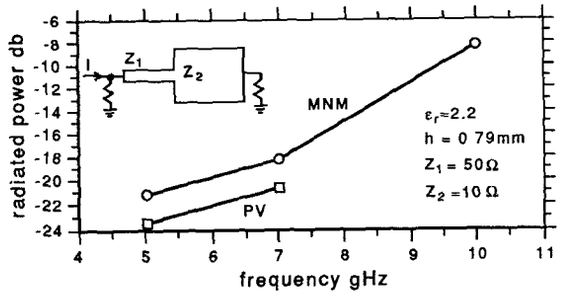

Figure 7. Normalized radiated power from a step (MNM: Multiport Network Model, and PV: Poynting Vector method [1]).

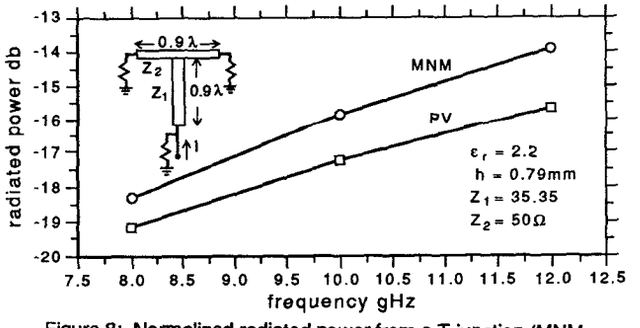

Figure 8: Normalized radiated power from a T-junction (MNM: Multiport network model, and PV: Poynting Vector method [1]).

Radiation from a Tee-Junction Discontinuity

Computed results for power radiated from a T-junction (50W main line with 35.35W branch line on a substrate thickness 1/32" and e_r = 2.2) are shown in Figure 8. The radiation loss at 12 GHz is 0.18 dB. It is found that for such a T-junction that most of the contribution to the radiation losses originates from the region of the junction.

Concluding Remarks

The results reported in this paper show that the multiport network model is a convenient and versatile method for evaluating radiation and spurious coupling associated with discontinuities in microstrip circuits.

Radiation losses from microstrip discontinuities cannot be neglected at higher frequencies. For a 10Ω to 50Ω step change (ε_r = 2.2, h = 0.79 mm) in width, the radiation loss at 10 GHz is 0.7 dB. For a 90° bend in 50Ω line on a 10 mil thick substrate with ε_r = 2.2, the radiation loss at 40 GHz is 0.17 dB. The multiport network model can be used for calculating radiation and coupling from complicated discontinuity configurations such as chamfered bends, compensated T-junctions and cross-junction. More detailed results will be reported at the meeting. Experimental verification is being planned.

Computation results are in good agreement with the Poynting vector method applicable for simple geometries.

This approach has been extended to computation of spurious coupling between two discontinuities in different parts of a microwave circuit. This algorithm is being implemented and numerical results will be presented at the Symposium.

References

[1] Lewin L., Proc. Inst. Elec. Eng.-117(C), 1960, pp.163-170.

[2] Lewin L., IEEE Trans. MTT-26, 1978, pp. 893-894.

[3] Lewin L., Proc. Inst. Elec. Eng.-125, 1978, pp. 633-642.

[4] Abouzahra M. and Lewin L., IEEE Trans. MTT-27, 1979, pp. 722-723.

[5] Abouzahra M.D., IEEE Trans. MTT-29, 1981, pp. 666-668.

[6] Hoffman R.H., chapter 11 in Handbook of Microwave Integrated Circuits, Artech House, 1987, pp. 311-321.

[7] Wolff I. et al., Electronic Letters-8, 1972, pp. 45-77.

[8] Menzel W. and Wolff I., IEEE Trans. MTT-25,1977, pp.107-112.

[9] Chadha R. and Gupta K.C., IEEE Trans. MTT-30, 1982, pp. 2151-2156.

[10] Maramis H.J. and Gupta K.C.,Sci. Rept. No. 96, EM Lab, University of Colorado, Boulder, 1988.

[11] Kompa G. and Mehran R., Electronics Letters-11(9), 1975, pp. 459-460.

[12] Benalla A and Gupta K.C., IEEE Trans. AP-36, 1988, pp. 1337-1342.

[13] Benalla A and Gupta K.C., IEEE Trans. AP-37,1989 (to appear).

[14] Benalla A and Gupta K.C., IEEE Trans. MTT-34, 1986, pp. 733-736.